The effects of weathering on the physical and mechanical properties of igneous and metamorphic saprolites

Rocchi, Irene; Coop, M. R.; Maccarini, M.

Published in:
Engineering Geology

Link to article, DOI:
10.1016/j.enggeo.2017.10.003

Publication date:
2017

Document Version
Peer reviewed version

The effects of weathering on the physical and mechanical properties of igneous and metamorphic saprolites

I. Rocchi[a,1], M.R. Coop[b] & M. Maccarini[c]

[a]Department of Civil Engineering, Technical University of Denmark, Brovej, Building 119, 2800 Kgs. Lyngby, Denmark, formerly University of Bologna.

[b]University College London, Gower St, London WC1E 6BT, United Kingdom, formerly City University of Hong Kong

[c]Department of Civil Engineering, Universidade Federal De Santa Catarina, Rua João Pio Duarte da Silva, s/n Córrego Grande, Florianópolis - SC, 88040-900, Brazil.

[1] Corresponding author: ireroc@byg.dtu.dk

Abstract

The present paper presents three extensive datasets of laboratory testing on weathered geomaterials, which are emblematic of soil types widely found worldwide. The overall dataset includes soils originating from igneous and metamorphic rocks, either coarse or fine grained and having either felsic or mafic minerals. In particular, the data are interpreted to highlight the effects that weathering has on the physical and mechanical properties of these natural geomaterials comparing them with published data with the aim to provide a general framework of interpretation that takes into account this geological process and links soil mechanics to engineering geology. Generally, weathering induces a reduction in the grain size, both due to physical actions (e.g. opening of grain contacts) and to the chemical decomposition of minerals resulting in the formation of clay minerals. As weathering proceeds and the soil becomes finer, the in situ specific volume and the location of the normal compression and critical state lines move upwards in the volumetric plane. On the other hand, the clay minerals cause its angle of shearing resistance to reduce. When analysing the behaviour of the intact soil, in all cases positive effects of structure, albeit small compared to some sedimentary soils, were observed and these reduced as a consequence of weathering.

Key words

Residual soils, saprolite, structure, weathering

Introduction

Although weathering is an inherent process undergone by any material, in the geotechnical community, this geological process tends to be associated particularly with certain climates. This is true to the extent that for long “tropical soil” has been used as a synonym of residual soil and indeed the geomaterials presented here are from tropical areas. However, as explained by Hall et al. (2012), climate merely influences the rate at which weathering occurs, while the specific processes involved are dictated by the parent rock characteristics, such as

porosity and permeability, pre-existing joints and bedding planes, mineralogy and mineral properties.

Extensive research exists that has investigated changes of physical properties and mineralogy along weathered profiles. However, as pointed out by Moon & Jayawardane (2004) it is often difficult to measure meaningful mechanical parameters across the whole weathering profiles as the material investigated can span from a hard rock to a soft soil. For this reason the present paper focuses on the "soil end" of the weathering spectrum, i.e. saprolites and residual soils, where the fundamental concepts of soil mechanics can be applied.

Vaughan et al. (1988) were perhaps the first to investigate the effects of structure on the mechanics of natural residual soils within a critical state framework. A work that was further extended to other natural soils and rocks by Leroueil & Vaughan (1990), who recognised the importance of natural structure irrespective of its geological origin, while previous work had concentrated almost solely on its effects for sedimentary "sensitive" clays (e.g. Skempton, 1970). After these pioneering studies, more recently Futai et al. (2004) investigated in detail the mechanical behaviour of an intact saprolite comparing it to that of the recompacted soil at different depths along a weathered profile. However, a well-established framework of behaviour like that proposed by Cotecchia & Chandler (2000) for natural sedimentary clays that includes the effects of structure is still lacking for geomaterials originated from weathering.

The current paper aims at establishing the basis for such a general framework of interpretation and improving the understanding of the weathering effects on the geotechnical behaviour, linking the latter to the geological processes that have occurred. The effects of weathering on the physical and mechanical properties of a granitic saprolite from Hong Kong, a gneissic saprolite from Brazil and a basaltic saprolite from Mauritius are discussed. In particular, profiles of significant depth and having a variety of weathering degrees are

considered. These data are compared with published data regarding weathered geomaterials, which were reanalysed applying the critical state and sensitivity frameworks. Finally, the trends of behaviour were contrasted with the influence of weathering on a sedimentary clay.

Materials and testing procedures

Three types of soil were considered in detail, making comparisons and contrasts with examples from the literature that were of broadly similar materials. Table 1 summarises the soil properties, the test data available the and main findings for each case. This information is also presented in Figs. 1-3, plotted against depth. Because both physical and mechanical properties are included to aid a global understanding at a glance, this will require reference to these figures in different sections of this paper. Figure 1 compares a granitic saprolite from Hong Kong to a diabase saprolite from Santa Catarina (Brazil), as both parent rocks have an igneous intrusive origin, but differ in mineralogy and partly in grain size. Figure 2 compares two gneissic saprolites from Brazil (Rio de Janeiro and the State of Minas Gerais, respectively), which share the same geological origin and approximately the same grain size and mineralogy, although it is not clear whether the geological formation considered is indeed the same one. Figure 3 compares a basaltic saprolite from Mauritius to a volcanic ash residual soil from Java (Indonesia), as both parent rocks are extrusive igneous rocks, but they differ in mineralogical composition.

As mentioned above, the first soil considered (Fig. 1) is a granitic saprolite from Hong Kong. According to the guidelines of the Geological Society Working Party (1990), the soil has grades IV (highly weathered) and V (completely weathered). The parent rock (Sha Tin Granite) is an intrusive coarse to fine grained felsic igneous rock, having crystal sizes between 1 and 4mm with plagioclase, feldspars, quartz, and to a lesser extent biotite as the main mineral components. The soil was sampled from two boreholes (BHA and BHB) located at a close distance, covering depths up to 27m. A variety of different weathering degrees were

encountered, which are detailed in Table 2, based on Rocchi & Coop (2015). However, for simplicity in Fig. 1, distinction is made only between the two decomposition grades, i.e. CDG and HDG that stand for Completely Decomposed Granite and Highly Decomposed Granite, respectively. Furthermore, the tests presented will focus on the shallow extremely weak CDG (sh ewCDG) and HDG, which represent the extremes encountered.

For the granitic saprolite several one-dimensional compression and triaxial tests were carried out, both on intact and reconstituted samples, using the techniques described in detail by Rocchi & Coop (2015). The soil gradings in Fig. 1a (and similarly in Figs. 2a and 3a) are presented by dividing the particle size distribution curves into their main components, i.e. gravel, sand and fines (silt and clay). As several grading curves were available at similar depths, the values were averaged over 0.5-1m intervals. The soil ranges from sandy gravel to gravelly sand (D_{max}=6-20mm and D_{50}=1-11mm) so that the soil grains mostly include clusters of different minerals. Generally, the shallower and more weathered the soil, the finer and better graded. However, below 12m a larger data scatter in the relative amounts of gravel and sand can be observed. This rather regular alternation between more and less weathered strata could be an indication of the joint spacing. In addition, at approximately 20m depth a more weathered stratum was encountered, as shown by the increased amount of fines. Rocchi & Coop (2015) described this granitic saprolite mineralogy as consisting mainly of quartz and feldspars in similar amounts, and to a lesser extent of mica, clay minerals (kaolinite and illite) and some amorphous minerals. Compared to the parent rock, amorphous and clay minerals have replaced the biotite and to a lesser extent the feldspars due to weathering. This is reflected in the specific gravity (G_s), which is 2.65 for the HDG and on average 2.63 for the CDG.

The gradings of a diabase saprolite from Santa Catarina (Brazil) studied by Maccarini et al. (1989) are included in Fig. 1a for comparison as it differs from the granitic saprolite in mineralogy and partly in grain size. This saprolite was from a shallow intrusive medium

grained mafic igneous rock, more commonly known as dolerite. The samples (D1 to D4) belong to a saprolitic layer found at a few metres depth under a highly weathered layer, most likely meaning that they correspond to grade V. In this case, there were no triaxial tests; oedometer tests on intact specimens were carried out at all the depths sampled, while only samples D1 and D4 were tested in a reconstituted state. As seen in Fig. 1a, the doleritic saprolite is finer than the granitic saprolite, partially due to the parent rock grain size, but possibly also because of the shallower depth. This soil ranges from silty sand to sandy silt, with very small amounts of clay and gravel for the deeper samples (D_{max}=2-5mm), as can be seen in Table 1. However, the soil becomes again finer towards the surface. Although the exact variation with depth of the mineralogical composition of the parent rock and that of the doleritic saprolite are unknown, the main minerals are feldspars (65-70%), pyroxene (25%) and to a lesser extent magnetite (5%). This is responsible for higher G_s than in the granitic saprolite, which range from 2.98 to 3.07.

The second soil considered (Fig. 2) is a gneissic saprolite from Rio de Janeiro (Brazil), which was block sampled both along an excavation front (T06 to T01) and inside a well (P01 to P05) up to an overall depth of about 14m. The parent rock characteristics prior to metamorphisation are unknown, but gneiss indicates a medium to coarse grain size for the fresh rock. The saprolite is stratified due to metamorphisation, with thicknesses from a few cm to several tens of cm. Except for the uppermost level (T06), which corresponds to grade VI (residual soil), the soil is a grade V saprolite. Several oedometer and triaxial tests were carried out on intact specimens for samples below 5m depth, but not on the reconstituted soil. In particular, four drained triaxial tests were carried out for each of these samples with confining pressures between 50 and 400kPa. Two identical tests were carried out for each sample and as their results were almost identical, average lines are presented.

In Fig. 2a the data are presented calculating the depth with respect to the top of the excavated slope and the soil sampled along the face (i.e. the samples with the prefix T) can be considered overall more weathered. The soil is a sand with little fines and as can be seen in Table 1, D_{max} is approximately 4mm for all samples, while D_{50} is 0.2 to 0.4mm. Between 0m and about 2m the soil consists mostly of clay (66%), but otherwise the clay fraction is rather low (5%). Despite a possible sedimentary origin of the rock before metamorphism, the soil is well graded (c_u=27-141). The profile of mineralogical composition with depth is unknown, but around 60-90% of the minerals are feldspars, 10-40% quartz and less than 5% mica. The G_s values range between 2.73 and 2.79, consistently with the acidic composition of the mineralogy.

The gneissic saprolite investigated by Futai et al. (2004) covers grade VI from 0 to 2m (Horizon B) and V (Horizon C) below that. Triaxial tests were carried out on samples every 1m concentrating at 1 and 5m depth, which are identified as Horizon B Gneiss (HBG) and Horizon C Gneiss (HCG), respectively. In Fig. 2a, the sand fraction is considerably less than for the gneissic saprolite studied, while the clay fraction is similar. Interestingly, the silt component almost disappears close to the surface, which is also observed in sample T06, possibly because of the resistance to chemical weathering of sand sized quartz minerals. The mineralogy consists mainly of quartz (45%), kaolinite (35%) and other minerals (5-10%). However, within grade VI the kaolinite content reduces, while gibbsite and iron oxides increase. For this gneissic saprolite the G_s values are slightly lower, ranging from 2.68 to 2.63 towards the surface.

The third soil considered (Fig. 3) is a basaltic saprolite from Mauritius, which has already been described to some extent by Vaughan et al. (1988) and originated from an extrusive mafic igneous parent rock. Two units were block sampled at 8 and 30m, which are identified as strong basalt (SB) and weak basalt (WB) and could correspond to grades IV and

V, respectively. Five triaxial tests were carried out for the WB soil and seven for the SB, and for each sample one specimen underwent shear at a low stress. At both depths the soil is composed in nearly equal parts of sand and fines (about 40%) with a small gravel component (Fig. 3a), D_{max} being 5mm. Compared to the previous examples, the change in grading between the two depths is minimal, although it is still possible to observe that the soil becomes slightly finer as weathering increases. The plasticity limits are independent of depth and PI=5% (Fig. 3b). It is interesting to note that the natural water content w_n is within the plastic range for the SB, while it is clearly above for the WB, but the values correspond to 80-90% degree of saturation. The allophane rich volcanic ash tuff from Java (Indonesia) originated from an extrusive felsic igneous parent rock. Wesley (1990) carried out oedometer tests on the intact and reconstituted soil, in the latter case remoulding the sample at its natural water content and around its liquid limit. While the basaltic saprolite has almost no clay, as seen in Table 1, this soil is a much finer silty clay (60% clay) that has reached weathering grade VI. In addition, due to the allophane minerals it has an extremely high plasticity in its natural state. For the basaltic saprolite and the volcanic ash residual soil in Fig. 3c, the in-situ specific volume (v=1+e), v_0 follows a trend similar to w_n in Fig. 3b, increasing towards the surface.

Figure 4 compares all soils using more general classes, such as igneous and metamorphic origin, coarse and fine graded, and felsic and mafic mineralogy. For this "summary figure" (and Figure 12 later on) circles represent igneous parent rocks and triangles metamorphic ones, while solid and empty symbols represent coarse and fine grained parent rocks, respectively. In addition, continuous and dotted lines represent felsic and mafic mineralogy, respectively. For example, empty circles and solid lines would represent data points for a felsic igneous fine parent rock. It should be pointed out that not all the possible combinations are present.

The speed at which weathering progresses depends on the climate, topography, joint spacings and orientations and other properties of the parent rocks. It is therefore quite surprising to see that the same weathering grades are achieved at similar depths for different parent rocks and weathering environments. In particular, grade VI is reached at very shallow depths (about 2m) both in the saprolites having metamorphic parent rocks and in the igneous doleritic saprolite. In addition, although Wesley (1973) reported the volcanic ash residual soil as consisting of a uniform layer, it is clear in Fig. 4b and c that the first 2m of the profile identify a rather different unit. Coincidentally, this is also a common value for the depth of the desiccation crust encountered in sedimentary clays. At this shallow depth biogenic action is likely to play a major role. In addition, ground water fluctuation and temperature excursions are greatest within the first few metres of soil.

With regards to the boundary between grade IV and V, this is at or below 25m for the granitic and the basalic saprolites. Abad et al. (2016) identified a prevalence of horizontal and vertical joints, respectively, in the completely and highly weathered granite from Malaysia they analysed. It is possible that the horizontal joints caused by stress relief (i.e. unloading) play a role in determining the thickness of this weathered layer as they tend to have limited occurrence at depth, although other sets of joints, such as cooling or tectonic joints, also contribute to increasing water permeability and therefore the rate of weathering.

The limited changes in G_s described earlier show that the influence of the initial mineralogical composition is rather strong. Although similar overall trends are followed, the gradings are very different as seen in Fig. 4a where only the division between coarse and fine components (i.e. a 2mm threshold) is taken into account. The gradings of the saprolites having igneous parent rocks do not share the same amount of coarse or fine components and seem not influenced so much by their intrusive or extrusive origin, i.e. the original grain size. The basaltic saprolite and the volcanic ash residual soil, whose parent rock grain sizes would be the

closest before weathering, are the case where the difference in current particle size is the greatest. On the other hand, the basaltic and doleritic saprolites, which are both mafic, appear to have a similar coarse to fine ratio. For the metamorphic saprolites the gradings are surprisingly different given their close location and shared geological origin. When looking at each individual set of data separately, generally the coarser grained materials derived either from igneous or metamorphic rocks show a reduction in the grain size towards the surface (i.e. increasing weathering). In these cases, the fines increase considerably only at very shallow depths. On the other hand, fine grained soils do not appear to show significant changes in their grading. As can be seen in Table 1, these soils are generally well graded, but the gneissic saprolites may become gap graded at the final stages of weathering.

In Figure 4b, the natural water contents and liquid and plastic limits are presented. The fines resulting from mafic rocks appear to be more plastic than those from felsic rocks. However, the fine and even more so the clay fraction are small for the majority of these soils. The only exception is the volcanic ash residual soil, which has very high plasticity indeed. Wesley (1973) attributed this to the presence of allophane minerals, which are meta-stable, so that if the soil is allowed to dry the clay content falls below 20%.

Compression Behaviour

One-dimensional Compression

Figure 5a shows the oedometer tests carried out on intact specimens of the granitic saprolite, where results from K_0 stress-path tests were used to calculate p'. The compression tests for reconstituted specimens, which define the one-dimensional Normal Compression Line (1D-NCL*), are not included here for brevity, but can be found in Rocchi & Coop (2015). With regard to the intact samples (grey lines in Fig. 5a), the more weathered unit (sh ewCDG) has an extremely gradual yield, while the less weathered unit (HDG) only begins to yield at the maximum stress applied. The change of the 1D-NCL* location in the volumetric plane with

weathering is shown in Fig. 1b and 1c, relating its intercept at 1kPa N_0 and its slope λ to depth, as was already done for the physical properties. Both parameters generally increase towards the surface, but are lowest close to the ground surface. Figure 1b also shows the specific volume in situ (v_0), which is approximately constant and rather low at depth, resulting in very low compressibility for the HDG. The v_0 values then increase towards the surface following a consistent trend despite some locally more weathered units. This is responsible for the larger compressibility of the sh ewCDG.

The 1D-NCL* moves upwards in the volumetric plane also for the doleritic saprolite presented for comparison, as both N_0 and λ increase towards the surface based on the oedometer tests carried out on reconstituted samples D1 and D4 (thick lines in Fig. 6a). However, a direct comparison is not easy as the depth ranges covered by the granitic and doleritic saprolites overlap only slightly. Both N_0 and λ have higher values for the doleritic saprolite, due to a finer particle size and higher plasticity, although this soil is better graded. Due to the same reasons, the intact doleritic saprolite also has larger v_0 in Fig. 1b. After an initial increase in the early stages of weathering, v_0 is rather constant along the profile. Higher v_0 values cause the doleritic saprolite to yield rather sharply compared to the granitic saprolite during compression (Fig. 6a).

Figure 6b compares the tests for the intact doleritic saprolite samples in the Void Index plane, as defined by Burland (1990). The void index ($I_v=(e-e^*_{100})/c_c^*$) normalises the compression curves of intact samples with respect to the 1D-NCL* gradient (c_c^*) and its intercept at 100kPa (e^*_{100}), when a logσ'_v rather than a logp' axis is used, and where the * indicates that it is the NCL for the reconstituted soil. This line, called the ICL by Burland, has been assumed to be straight over the relatively narrow range of stresses used in the tests, not curved as assumed by Burland for clays over a wider stress range. The tests for the doleritic saprolite in Fig. 6b cross the ICL, which indicates positive effects of structure. As oedometer

tests were carried out only for samples D1 and D4 on reconstituted specimens, it was assumed that the 1D-NCL* was the same for samples D3 and D4, based on their gradings and Atterberg limits and similarly for samples D1 and D2. Yielding occurs at around the overburden pressure and then, at least to some extent, the curves converge towards the ICL. Sample D2 travels the greatest distance outside the ICL, therefore showing the greatest effects of structure, but after yielding the slope of the compression path is the steepest indicating the greatest structure degradation. This large difference might be to some extent an artefact of using the same ICL for samples D1 and D2, despite some differences in their physical properties.

To quantify the effects of structure the stress sensitivity S_σ as defined by Cotecchia & Chandler (2000) was used. This is defined as the ratio between the yield stress (σ'_y) and an equivalent pressure (σ'^*), which is taken as that pressure on the ICL which has the same specific volume as that on the intact compression path at yield σ'_y. As the soil presents a positive effect of structure $S_\sigma>1$ and high S_σ indicate a highly metastable and possibly cemented state in situ.. In Fig. 1e S_σ values have a rather limited range, except sample D2 for the reasons already mentioned. S_σ is overall only slightly larger for the doleritic saprolite than for the granitic saprolite, for which selected normalised results are showed in Fig. 7a that compares the granitic and doleritic saprolites in the Void Index plane. Only samples D1 and D4 are included here to avoid overcrowding and because reconstituted tests were carried out on these samples, making their data interpretation more reliable. The data from Wesley (1990) and Cafaro & Cotecchia (2001) are also presented for comparison, but the original curves in a traditional volumetric plane are not included here for brevity, as they are available elsewhere.

Examining Fig. 7a it appears that the granitic saprolite is the most susceptible to the effects of weathering, as the initial I_v values cover the widest range. This difference might be justified upon comparison with the doleritic saprolite due to a wider range of depth being investigated. However, the effect is very large indeed compared to the sedimentary clay tested

by Cafaro & Cotecchia (2001), where the samples were also taken several metres apart. This may suggest that the coarser the soil, the greater the effect of weathering. No comment can be made in this regard for the volcanic ash residual soil, as oedometer tests were only available for one weathering degree.

The more weathered granitic saprolite (sh ewCDG) and the doleritic saprolite have similar I_v initially and plot close to the ICL. However, yielding is much more gradual and starts earlier for the sh ewCDG. In addition after reaching beyond the ICL, the sh ewCDG curve remains parallel to it. On the other hand, the doleritic saprolite has a clearer yield and converges slightly onto the ICL afterwards, which indicates a micro-structure that is more easily broken down by strain. The volcanic ash residual soil is the only soil with an initial state that plots above the ICL and shows a sharp yield point to then converge quickly onto the ICL. When comparing these results with the behaviour of the sedimentary clay, it can be seen that both the weathered and fresh clay, termed the yellow and grey clay by Cafaro & Cotecchia (2001), typically have a much lower in-situ value of I_v. The amount by which they reach out beyond the ICL is similar to other soils in that region of I_v and similarly the compression paths remain parallel to the ICL after yield. The least weathered granitic saprolite (HDG), whose starting point is the furthest from the ICL, only just starts to yield at the highest stress achieved, therefore showing the greatest effects of structure. Except for the HDG, yielding occurs around the overburden pressure, but there is no full convergence to ICL within the stress level tested. In most cases, the curves actually remain parallel to the ICL and overall, for igneous saprolites the finer the soil the sharper the yield and the greatest the convergence towards the ICL. In addition, for the igneous saprolites I_v is higher for the most weathered samples and the compression curves reach further beyond the ICL, while the opposite is true for the sedimentary clay. Sensitivity values were also compared for all these soils, but will be discussed later together with results from isotropic compression.

As in many cases the focus was on triaxial tests, a modified version of the normalising parameter v_n proposed by Coop & Cotecchia (1995) was also used to interpret the data, but using the Critical State Line (CSL) as reference. This parameter is defined as the current distance from the CSL on a lnv:lnp' plane, so that $v_{n,CS}=\exp((\ln(v)-\Gamma)/\lambda)$, where Γ is the CSL intercept at 1kPa on a lnv:lnp' plane and λ its slope. The CSL was used here as a reference line because the isotropic NCL* was not available for most cases. Furthermore, the CSL was assumed to be straight and parallel to the 1D-NCL* within the pressure ranges tested/analysed. Besides generally providing a good fit, this assumption simplified the normalisation. When using the CSL as a reference, the usual definition of positive and negative effects of structure, according to whether or not the ICL is crossed loses meaning, since the compression path must cross the CSL, provided sufficient stress is applied. However, the magnitude of structure can be measured using the maximum distance from the CSL. This is independent of the spacing between the NCL and CSL, which can change with the soil type. In Fig. 5b the oedometer tests obtained for the granitic saprolite are interpreted in terms of $v_{n,CS}$. The compression paths of the sh ewCDG remain approximately parallel to the CSL after yield, while the HDG again only just starts to yield at the maximum stress achieved, similarly to the I_v plot (Fig. 7a).

In Figure 8a and b the one-dimensional compression tests (samples T04, T02, P01, P02, P03, P04 and P05) are shown for the gneissic saprolite with dashed lines in a traditional and in a normalised plane, respectively, where results from K_0 stress-path tests were used to calculate p'. There does not really seem to be any trend linking the initial $v_{n,CS}$ values with weathering degree, but generally the starting location is on the left hand side of CSL and the compression paths reach a clear yield within the pressure range tested. After yield the compression paths usually have a slope greater than the CSL, but converge only slowly with it, indicating a slow rate of destructuration. When considering only the most (T04) and least (P05) weathered samples, the former shows signs of yield earlier and more gradually. After crossing the CSL, the curve remains parallel and very close to it. Sample P05 instead yields after the in situ stress

and moves further beyond the CSL. A difference in soil fabric could be the explanation, as v_0 in Fig. 2b is lowest at depth, increases until about 10m depth and then remains approximately constant up to the soil surface. Note that the horizontal step in v_0 is due to samples P01 and T02 having the same depth with respect to the original excavation front. The gneissic saprolite studied by Futai et al. (2004), which covers a more limited depth range, also has rather constant v_0 in a similar range, but experiences a larger increase close to the soil surface (Fig. 2b). The compression results for this soil will be discussed later as only isotropic tests were available.

The tests on the gneissic and granitic saprolites are compared in Fig. 7b, where only samples T04 and P05, are included for clarity. The distance between the curves of different weathering degrees remains the largest for the granitic saprolite. For both saprolites the more weathered samples have higher $v_{n,CS}$ and yield more gradually, at around the overburden pressure. On the other hand, the less weathered samples reach further beyond the CSL and yield at stresses larger than the overburden pressure. In all cases, the compression paths remain parallel to the CSL after yield. For the sedimentary clay studied by Cafaro & Cotecchia (2001), $v_{n,CS}$ is higher for the least weathered sample and for both weathering degrees yielding occurs at stresses much higher than the overburden pressure.

Isotropic Compression

The isotropic compression tests on the granitic saprolite are shown in the traditional and normalised planes in Fig. 5a and b, respectively. Similarly to the oedometric tests, the curves show a very gradual yield that appears to be still ongoing at the maximum stress reached and therefore S_σ values cannot be calculated in this case. The data for the gneissic saprolites are presented in Fig. 8a and 8b and show a clearer trend compared to the oedometer tests. In particular, the shallowest sample (P01) plots higher and reaches a clear yield within the pressure range tested, but this is not so for the deepest sample (P05). In Fig. 8b all samples yield well after the overburden pressure and only sample P03 shows some convergence towards

the CSL. As already mentioned, v_0 is in the same range for the gneissic saprolite tested by Futai et al. (2004) and upon comparison with the results shown in Fig. 9a and b, the behaviour in compression is similar. As larger stresses were reached, both weathering degrees show clear yield, but slightly more gradually for the least weathered sample (HCG) and again the most weathered sample (HBG) plots above. In Fig. 9b it is clear that yielding is well after the overburden pressure and the degree of convergence towards the CSL is very limited. Figure 2e compares S_σ values for the gneissic saprolites. For the gneissic saprolite studied here, S_σ generally reduces towards the surface, while the opposite is true for the other gneissic saprolite.

Figure 10a and b show the isotropic compression tests for the basaltic saprolite. The tests on the weak basalt (WB) have similar v_0, except for the rogue value marked with a question mark, which does not reach the same CSL as identified by the other tests. All these tests show a clear yielding point in compression and thereafter the curves maintain constant slopes, showing a stable form of structure that cannot easily be broken down to give convergence. The strong basalt (SB) has lower and slightly more dispersed v_0 values and only the test that reached the maximum pressure shows signs of yielding. When looking at the normalised data, the WB yields at around the overburden pressure. In contrast, the deeper and less weathered SB does not show any sign of yield within the overburden pressure range. Again the more weathered sample plots above, but yield this time is sharper for the least weathered sample (SB).

The isotropic compression tests are compared in a normalised plane using $v_{n,CS}$ in Fig. 11, where selected tests have been included for each soil and only samples P01 and P05 from Fig. 8b for the gneissic saprolite. The difference between the most and least weathered samples is greatest for the granitic saprolite and smallest for the gneissic saprolite tested by Futai et al. (2004), the basaltic saprolite being an intermediate case. For both igneous and gneissic saprolites, the more weathered samples initially plot in the same area to the left of the CSL. All

of them start to experience yielding at around the overburden pressure and do not converge towards the CSL afterwards. The finer grained basaltic saprolite shows the sharpest yield.

The initial range of $v_{n,CS}$ values is very variable for the less weathered samples, but always below that of the more weathered samples. The granitic saprolite has the lowest $v_{n,CS}$ initial value and the gneissic saprolite studied by Futai et al. (2004) the highest. The gneissic saprolites just begin to yield within the overburden pressure range, but not the igneous saprolites. Again the basaltic saprolite shows the sharpest yield. In contrast, the least weathered sample plots above but relatively close to the more weathered sample of the sedimentary clay studied by Cafaro & Cotecchia (2001) and both samples yield at stresses much larger than the overburden pressure. These trends can be roughly explained by examining v_0 in Fig. 4c. There v_0 follows an overall trend for the saprolites increasing towards the surface, ignoring local fluctuations. Furthermore, the finer soils tend to have higher overall values. However, v_0 does not change significantly for the sedimentary clay and reduces slightly with weathering.

Figure 4d illustrates the effects of structure using again S_σ, where grey symbols distinguish oedometer results from the isotropic compression data. When calculating S_σ on the $v_{n,CS}$ plane, the values obtained are naturally slightly larger than those based on I_v, because the equivalent pressure is taken on the CSL, but the overall trends are unchanged. The S_σ values are also slightly lower for isotropic compression tests as seen from the gneissic saprolite, which however has a rather erratic behaviour. The basaltic saprolites reach the greatest S_σ, as the doleritic sample D2 was excluded from Fig. 4d because it showed suspiciously high values. As mentioned above, the HDG only started to yield at the maximum stress applied and this results in it not being possible to calculate S_σ, as it relies on there being a yield point in the compression path. Gasparre & Coop (2008), who tested sedimentary clays, pointed out that an apparent small effect of structure may be to some extent an artefact of the normalisation used and does not truly reflect a weaker structure. Indeed such approach does not account for the initial

distance from the ICL when calculating the effects of structure. In all cases where it was possible to calculate S_σ, this is larger than 1 and therefore the effects of structure are positive. Compared to the sedimentary stiff clay tested by Cafaro & Cotecchia (2001), the effects of structure observed are at least similar or in some cases greater. It is not entirely clear whether S_σ actually increases towards the surface for the saprolites, but for the sedimentary clay S_σ reduces from 2.4 to 1.5 as a result of weathering (Cafaro & Cotecchia, 2001).

Shear Behaviour

Figure 5a shows example CSLs proposed for the sh ewCDG and the HDG. While the HDG reconstituted and intact specimens identify a unique CSL, this is clearly not the case for the sh ewCDG, for which the intact specimens identify a CSL shifted from that of the reconstituted specimens, although the two lines appear to be parallel. A stable fabric is typically linked to this behaviour (e.g. Cuccovillo & Coop, 1999). While it is clear from Fig. 5a that the CSL moves upwards in the volumetric plane with weathering, the trend is not as clear when looking separately at Γ, the intercept at 1kPa on the v:lnp' plot, (Fig. 1b) or the CSL slope λ (Fig. 1c), once all the weathering degrees investigated are included. This is because the CSLs both shift and rotate. However, generally both Γ and λ increase towards the surface and with weathering. As only oedometer tests were carried out on the doleritic saprolite tested by Maccarini et al. (1989), λ is compared in Fig. 1c assuming that the 1D-NCL* and the CSL are parallel and, as already mentioned, it is rather larger for the doleritic saprolite. The M values (q/p' at critical state) shown in Fig. 1d, which were calculated based on the critical state strengths reported in Fig. 5c, generally reduce towards the surface and with weathering. Some local departures from this trend, as observed in Fig. 5c, are to be expected as weathering progresses preferentially along joints.

In Figure 5d the state boundary surfaces (SBS), obtained by normalising the stress paths in Fig. 5c with reference to stresses taken on the CSL ($p'^*_{CS}=1/v_{n,CS}$) are shown for the HDG

and sh ewCDG. Since M changes with weathering degree, q is also normalised by M, which brings the CSL to coordinates 1:1. The normalised stress paths of the reconstituted soils used to derive the intrinsic state boundary surface (SBS^*) are not shown for clarity. As can be seen in Fig. 5c tests at high confining stress were carried out only for the sh ewCDG, but from the data available the dry (left) side of the SBS^* identified by the HDG appeared to be the same as for the sh ewCDG. Due to the very high pressures required, the wet (right) side of neither the intact or intrinsic SBS could be identified. This results from a separation between the isotropic NCL and CSL that is much greater than for sedimentary soils. The sh ewCDG intact and intrinsic SBSs appear to join at the CSL, while at low p'/p'^*_{CS} values the intact HDG SBS plots higher than that for the sh ewCDG, showing greater effects of structure.

The critical states of each gneissic saprolite sample are indicated in Fig. 8c along with the CSLs chosen. Given the data scatter and the scarcity of tests it was decided to combine data from "adjacent" samples when the points reached at the end of shear were reasonably close together (T02 and T04, P01 and P02, P04 and P05). Given the limited axial strain reached in shear, most samples were still contracting at the end of the tests, except for the tests at low stresses on samples P04 and P05, which were dilating and therefore most likely also did not reach the critical state, because strain localisation would have been probable. The graph shows clearly that the CSL moves upwards in the volumetric plane as weathering progresses, with the exception of the CSL identified by samples P01 and P02 that plots the highest. Again, this trend is not shown as clearly when observing the profiles in Figs. 2b and c, where Γ and λ are plotted with respect to depth, as the CSLs both shift and rotate. The stress paths of each test are not presented in Fig. 8c, as they are conventional drained tests, but the CSLs obtained based on the critical state points presented identify an approximately constant M (Fig. 2d). The normalised shear data for the gneissic saprolites are presented in Fig. 8e, where unfortunately, the test results are not sufficient to draw a SBS for all the four weathering degrees identified. Therefore distinction was only made between samples from the excavation front (T) and the well (P). The

SBS for samples P in Fig. 8e is slightly larger than that identified by samples T, which are more weathered.

Futai et al. (2004) provided a set of values for Γ, λ and M every 1m along the whole 7m profile they investigated. In Fig. 9a the critical state points are shown for the HBG and HCG at 1 and 5m depth, where most tests were concentrated. Some scatter can be observed and the tests at very low pressures tail off towards the horizontal asymptote of the CSL. As a straight CSL is necessary for the purposes of normalisation, the CSLs were not the same as those identified by Futai et al. (2004) as data below 100kPa were disregarded, restricting the analysis to the straighter part at higher pressures. This provided λ and Γ values that were somewhat higher and therefore, only values for 1 and 5m depth, where the data provided justify the values chosen, are included in Figs. 2b-d. Similarly to the gneissic saprolite studied, it could be more reasonable to group results for samples taken at different depths, rather than have a set of parameters every 1m, unless the material were extremely heterogeneous. If only the two depths presented in Figure 9 are taken into account, the λ and Γ values increase with weathering similarly to other soils. Based on the data in Fig. 9c, M was chosen to be the same for HBG and HCG given the data scatter, which is consistent with what is observed for the other gneissic saprolite.

The normalised shear data for this gneissic saprolite are presented in Fig. 9d, where it is again evident that the least weathered sample (HCG) has a larger state boundary surface. Based on the isotropic compression tests shown in Fig. 9a, the triaxial test on the HCG having the largest confining stress (800kPa) should have reached the NCL, but the SBS does not seem to be well-defined on the wet side, or else it appears to be highly anisotropic, with a SBS that is quite peaked and asymmetrical in shape, unlike that for the HBG.

Figure 10a shows the triaxial test results for the intact basaltic saprolite. As already mentioned, in this case the CSL was taken as a reference, but the gradient of a compression

curve of a reconstituted sample, which is not shown, was used as a guide for determining its slope. A unique CSL was chosen in the v:lnp' plane for the two weathering degrees given that the degree of scatter was such as to render possible divisions doubtful. Again, as only oedometer tests were available for the volcanic ash residual soil used for comparison, λ is compared assuming that the 1D-NCL* and the CSL are parallel. As reported in Fig. 3d λ is much greater than the values encountered for the basaltic saprolite or any of the other soils. In contrast, the critical state ratio M is different for the two samples as can be seen in Fig. 10c, and reduces with weathering (Fig. 3e). The graphical results of the oedometer tests presented by Wesley (1990) for the residual soils from Java are not included for brevity, as their interpretation is rather straightforward. In Figure 10d the SBSs for the basaltic saprolite are presented. The deeper SB SBS is larger in size indicating a greater effect of structure. One test for the WB, which was identified as suspect, has been disregarded in choosing the SBS. Similarly to the gneissic saprolite tested by Futai et al. (2004), the SBS shape is rather different between the two weathering degrees and tends to be anisotropic for the least weathered soil, although to a lesser extent.

Figure 12 compares the CSL locations in the volumetric plane that for most of the soils move upwards with weathering, being the highest for the basaltic saprolite, which may hint to finer grading being a possible controlling factor. This trend with weathering is in contrast with the findings for the sedimentary clay studied by Cafaro & Cotecchia (2001), where Γ clearly reduces towards the surface. However, it is unclear whether λ and hence compressibility (since the NCL and CSL are assumed to be parallel) increases as a result of weathering. Nor does λ depend very clearly on the overall grain size. For the sedimentary clay the CSL slope λ remained constant, although if structure degradation is caused by breakage of bonds λ can change. With regard to the critical state stress ratio M (Fig. 4d), this does not seem to be strictly dependent on the soil mineralogy, nor the soil grading in broad terms. However, M generally reduces with increasing weathering.

All the SBSs are combined in Fig. 13, where the SBSs of the sedimentary clay studied by Cafaro & Cotecchia (2001) are added for comparison. As reconstituted samples were not tested in shear for the majority of these soils, it is not possible to confirm that they have positive effects of structure, as it is for the sedimentary clay. However, this appears to be confirmed for the granitic saprolite (sh ewCDG) as the parts of the SBSs that can be identified lie outside the SBS* of the reconstituted soil. It should be noted that this is true either if the CSL identified from tests on reconstituted or intact samples is used, which are not the same for the sh ewCDG, but for consistency of interpretation, the CSL identified by intact specimens was used as for the other soils. If the granitic saprolite is disregarded, as the whole SBS could not be identified, in all cases the SBS shapes and sizes are fairly similar for the more weathered materials (open symbols), including the sedimentary clay, the only exception being one of the gneissic saprolites. It is however more difficult to draw conclusions regarding the less weathered samples (solid symbols). The data suggest in all cases a larger size and possibly an anisotropic shape, which is progressively lost as a result of weathering.

Conclusions

Three extensive datasets of laboratory testing on saprolites obtained from igneous and metamorphic rocks having different geological origins were analysed, where both intact and reconstituted samples for at least two weathering degrees were tested. Their physical properties spanned from those of gravel to silty clays, generally with low plasticity. These data were also compared with similar cases from the literature, helping to reinforce some general patterns that may be identified. Overall a reduction in the grain size can be observed with increasing weathering and the particle size distribution of the coarser grained soils can vary from well- to gap-graded, while the finer graded soils do not change significantly in particle size or distribution. Mineral decomposition and the resulting increase in the clay content is substantial only at very shallow depths. As weathering proceeds and the soil grading becomes finer, the in situ specific volume and the location of the normal compression and/or critical state lines

generally move upwards in the volumetric plane, but the clay minerals cause the critical state stress ratio (or angle of shearing resistance) to reduce. When longer profiles are considered, local departures from this trend can be observed, as weathering typically does not proceed monotonically with depth, especially where jointed structures are present such as in granites. On the other hand, sometimes the variation is not particularly clear if only a short profile is considered.

The effects of weathering on the intact soil mechanical properties were studied comparing the intact behaviour in compression and shearing of samples having different weathering degrees. To account for the different soil properties, the tests on the intact soil were first normalised relative to their intrinsic behaviour, i.e. using tests on reconstituted samples or properties at the critical state. In some cases, the intact CSL was used as a reference to assess the effects of structure if tests on reconstituted soils were not available. For all the case studies, positive effects of structure were observed. During compression, yield did not always occur around the overburden pressure, but often at higher stresses and frequently a constant slope was observed afterwards, indicating robust effects of structure that are difficult to break down by straining. This is similar to what is observed for stiff clays (e.g. Hosseini Kamal et al., 2014), where fabric dominates behaviour, but unlike softer clays or weak sandstones (e.g. Smith et al., 1992; Coop & Atkinson, 1993) where bonding dominates, for which there is rapid post-yield convergence. In shear, the SBS size reduced with weathering and in cases of high anisotropy, this was reduced with weathering.

Acknowledgments

This work was fully supported by a grant from the Research Grant Council of the Hong Kong Special Administrative Region (HKSAR), China T22-603/15 N (CityU 8779012). The authors would like to express their gratitude to Dr. John Endicott from AECOM for kindly providing some of the samples tested.

References

Alavi Nezhad Khalil Abad, S.V., Tugrul, A., Gokceoglu, C., Armaghani Jahed, D., 2016. Characteristics of weathering zones of granitic rocks in Malaysia for geotechnical engineering design. Engineering Geology 200, 94-103.

Baudet, B.A., Stallebrass, S., 2004. A constitutive model for structured clays. Géotechnique 54 (4), 269-278.

Burland, J.B., 1990. On the compressibility and shear strength of natural clays. Géotechnique 40 (3), 329-378.

Cafaro, F., Cotecchia, F., 2001. Structure degradation and changes in the mechanical behaviour of a stiff clay due to weathering. Géotechnique 51 (5), 441-453.

Coop, M.R., Atkinson, J.H., 1993. The mechanics of cemented carbonate sands. Géotechnique, 43(1), 53-67.

Coop, M.R., Cotecchia, F., 1995. The compression of sediments at the archaeological site of Sibari. In: Proceeding of 11th European Conference on Soil Mechanics and Foundation Engineering, Danish Geotechnical Society, Lyngby, 19-26.

Cotecchia, F., Chandler, R.J., 2000. A general framework for the mechanical behaviour of clays. Géotechnique 50 (4), 431-447.

Cuccovillo, T., Coop, M. R., 1999. On the mechanics of structured sands. Géotechnique 49 (6), 741–760.

Gasparre, A., Coop, M. R., 2008. The quantification of the effects of structure on the compression of a stiff clay. Canadian Geotechnical Journal 45 (9), 1324–1334.

Geological Society Engineering Group Working Party, 1990. Tropical Residual Soils - Geological Society Engineering Group Working Party Report, Quarterly Journal of Engineering Geology and Hydrogeology 23, 4-101.

Futai, M.M., Almeida, M.S.S., Lacerda, W.A., 2004. Yeild, strength and critical state behaviour of a tropical saturated soil. Journal of Geotechnical and Geoenvironmental Engineering, ASCE 130 (11), 1169-1179.

Hall, K., Thorn, C., Sumner, P., 2012. On the persistance of “weathering”. Geomorphology 149-150, 1-10.

Hosseini Kamal, R., Coop, M.R., Jardine, R.J., Brosse, A., 2014. The post-yield behaviour of four Eocene-to-Jurassic UK stiff clays. Géotechnique, 64 (8), 620-634.

Leroueil, S., Vaughan P.R., 1990. The general and congruent effects of structure in natural soils and weak rocks, Géotechnique 40 (3), 467-488.

Maccarini, M., 1987. Laboratory Studies of a Weakly Bonded Artificial Soil. Ph.D., Imperial College of Science and Technology, London, UK.

Maccarini, M., Texeira, V.H., Triches, G., 1989. Bonding properties of a residual soil derived from diabase. In: Proceeding 12th International Conference on Soil Mechanics and Foundation Engineering, Balkema, Rotterdam, pp. 525-528.

Moon, V., Jayawardane, J., 2004. Geomechanical and geochemical changes during early stages of weathering of Karamu Basalt, New Zealand. Engineering Geology 74, 57-72.

Rocchi, I., Coop, M.R., 2015. The effects of weathering on the physical and mechanical properties of a granitic saprolite. Géotechnique 65 (6), 482-493.

Skempton, A.W. 1970. The consolidation of clays by gravitational compaction. Quarterly Journal of the Geological Society of London, 125, 373-412.

Smith, P.R., Jardine, R.J., Hight, D.W., 1992. The yielding of Bothkennar clay. Géotechnique, 42 (2), 257-274.

Vaughan, P.R., Maccarini, M., Mokhtar, S.M., 1988. Indexing the engineering properties of residual soil. Quarterly Journal of Engineering Geology 21, 69-84.

Wesley, L.D., 1973. Some basic engineering properties of hallosyte and allophane clays in Java, Indonesia. Géotechnique 23 (4), 471-494.

Wesley, L.D., 1990. Influence of structure and composition on residual soils. Journal of Geotechnical and Geoenvironmental Engineering, ASCE 116 (4), 589-603.

Tables

Soil		**1**	**2**	**3**	**4***	**5+**	**6†**
Parent Material		granite	gneiss	basalt	dolerite	gneiss	volcanic ash
Depth (m)		6-40	2-14	8-30	2-9	1-7	1-10
	Dmax (mm)	6-20	2-9	5	2-5	U	U
	D_{50} (mm)	1-11	0.002-0.040	0.06-0.26	0.04-0.73	0.03-0.25	U
	c_u	5-32	27-141	47-52	29-89	6-30	n.a.
	clay fraction (%)	0-13	5-66	0-2	2-10	4-46	45-87
	PI (%)	n.a.	n.a.	5	14-18	16-29	13-65
	w_n (%)	5-23	12-21	40-76	31-42	26-46	47-67
	1D Compression	R and I	I	R	R and I	-	R and I
	Isotropic Compression	R and I	I	I	-	I	-
	Tiaxial shear	R and I	I	I	-	I	-
	Reference line	CSL	CSL	CSL	1D-NCL	CSL	1D-NCL
	v_0	1.4-2.0	1.71-2.20	2.30-2.56	2.23-2.74	1.88-2.34	2.61-4.54
	N and Γ	2.30-2.75 and 2.27-2.58	n.d. and 2.33-3.64	n.d. and 2.74	2.77-3.49 and n.d.	2.90-3.20	8.56 and n.d.
	λ	0.10-0.15	0.10-0.29	0.27	0.14-0.21	0.21-0.23	0.76
	M	1.28-1.53	1.54-1.57	1.42-1.75	n.d.	1.15	n.d.
	e_0	Incr	Incr	Incr	Incr	Incr	Incr
	N, Γ and *λ*	Incr and decr	Incr	None	Incr	Incr	n.d.
	M	Decr	None	Decr	n.d.	None	n.d.
		+ve	+ve	+ve	+ve	+ve	+ve
		Decr	Decr	Decr	Decr	Decr	Decr

Table 1 Summary of the soils properties, tests and effects of weathering for the weathered soils studied. Note: U stands for unknown, R for reconstituted, I for intact, Incr for increasing, Decr for decreasing and n.d. for not determined. *Data from Maccarini et al. (1989), +data from Futai et al. (2004) and †data from Wesley (1973, 1990)

Soil description	**Weathering grade**	**Acronym**	**Depth** (m b.g.l.)
extremely weak CDG	V	sh ewCDG	6.5-12 (BHA)
extremely to very weak CDG	V	evwCDG	12-20.5 (BHA)
extremely weak CDG	V	dp ewCDG	20.5-24 (BHA)
HDG	IV	HDG	24-27 (BHA) and 5.8-6.3 (BHB)

Table 2 Depths of the samples of Hong Kong granitic saprolite tested and the acronyms used. Note: CDG stands for Completely Decomposed Granite, HDG for Highly Decomposed Granite and BH for borehole

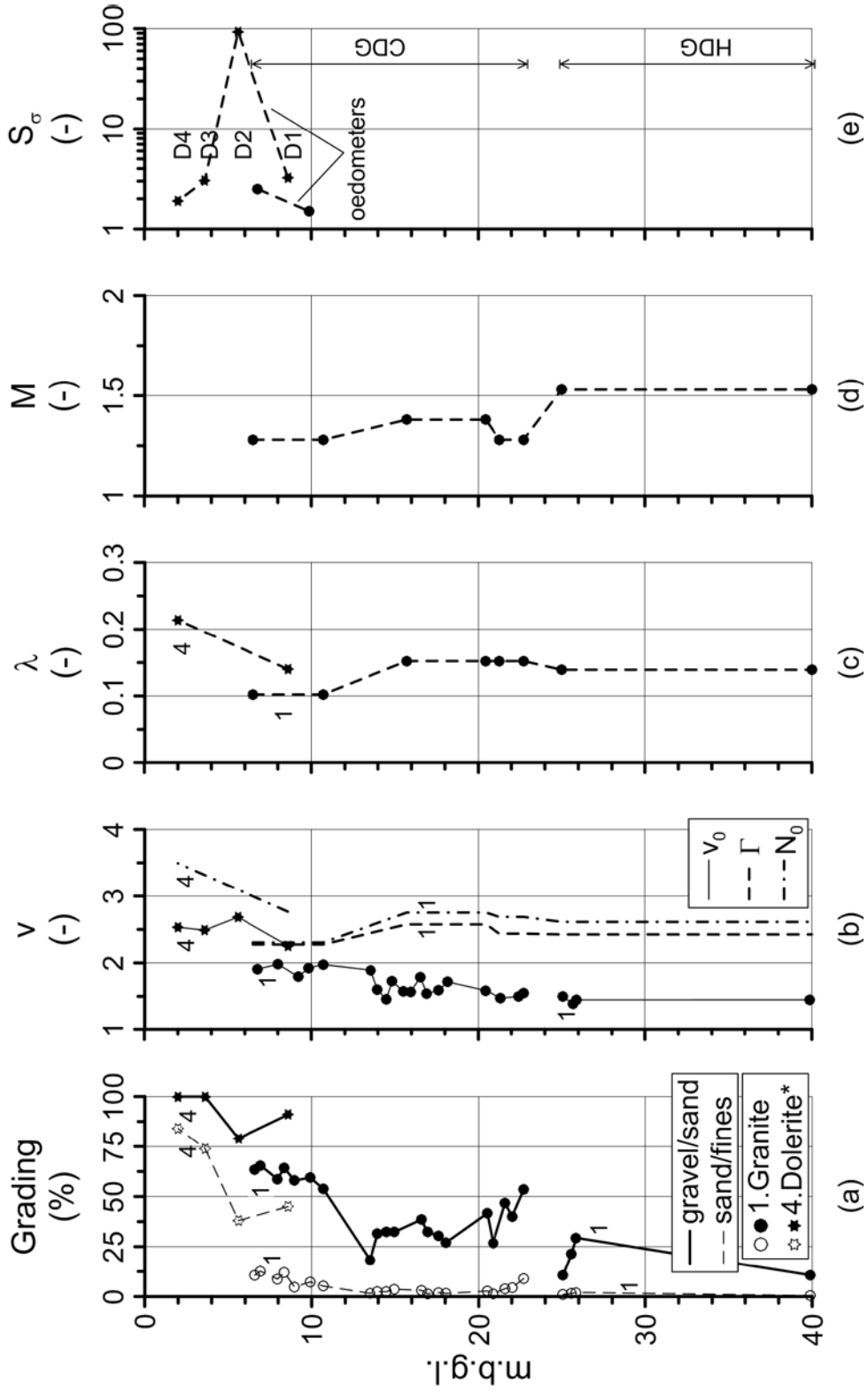

Figure 1: Comparison between the physical and mechanical characteristics of a granitic saprolite from Hong Kong (1) and a doleritic saprolite from Brazil (4). *Data from Maccarini et al. (1989)

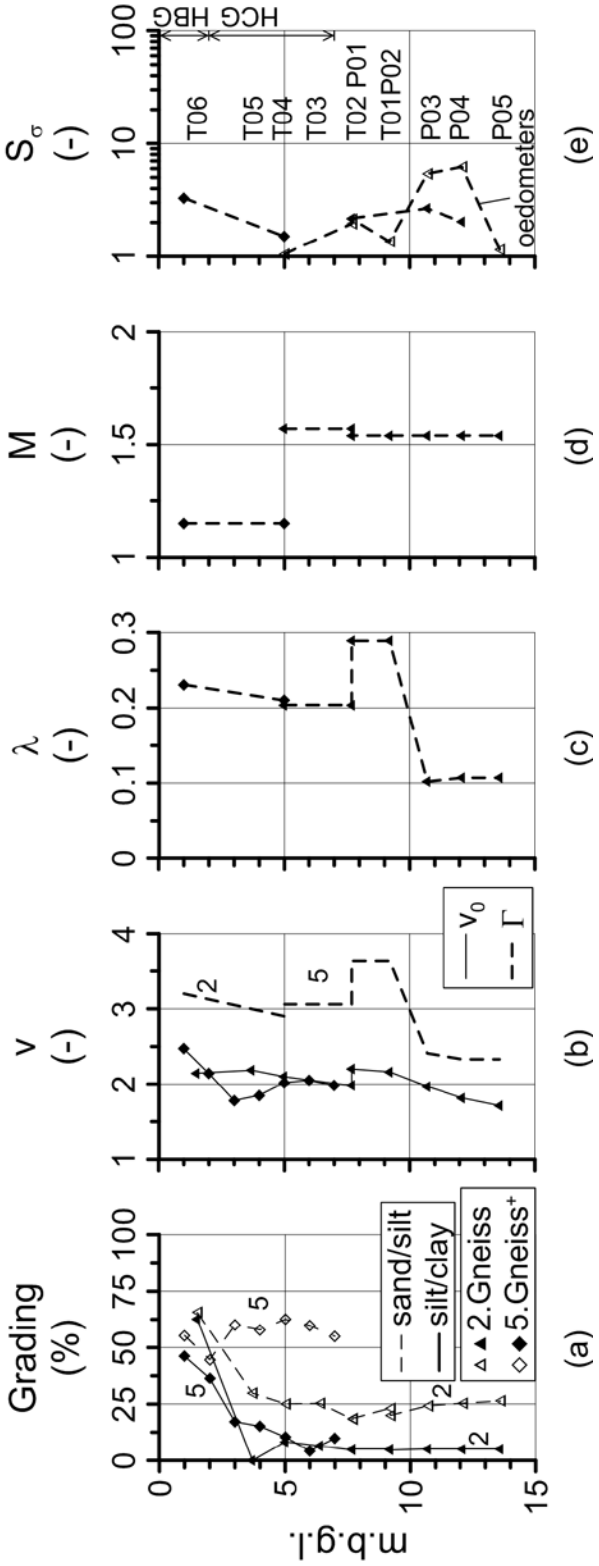

Figure 2: Comparison between the physical and mechanical characteristics of two gneissic saprolites from Brazil. [+]Data from Futai et al. (2004)

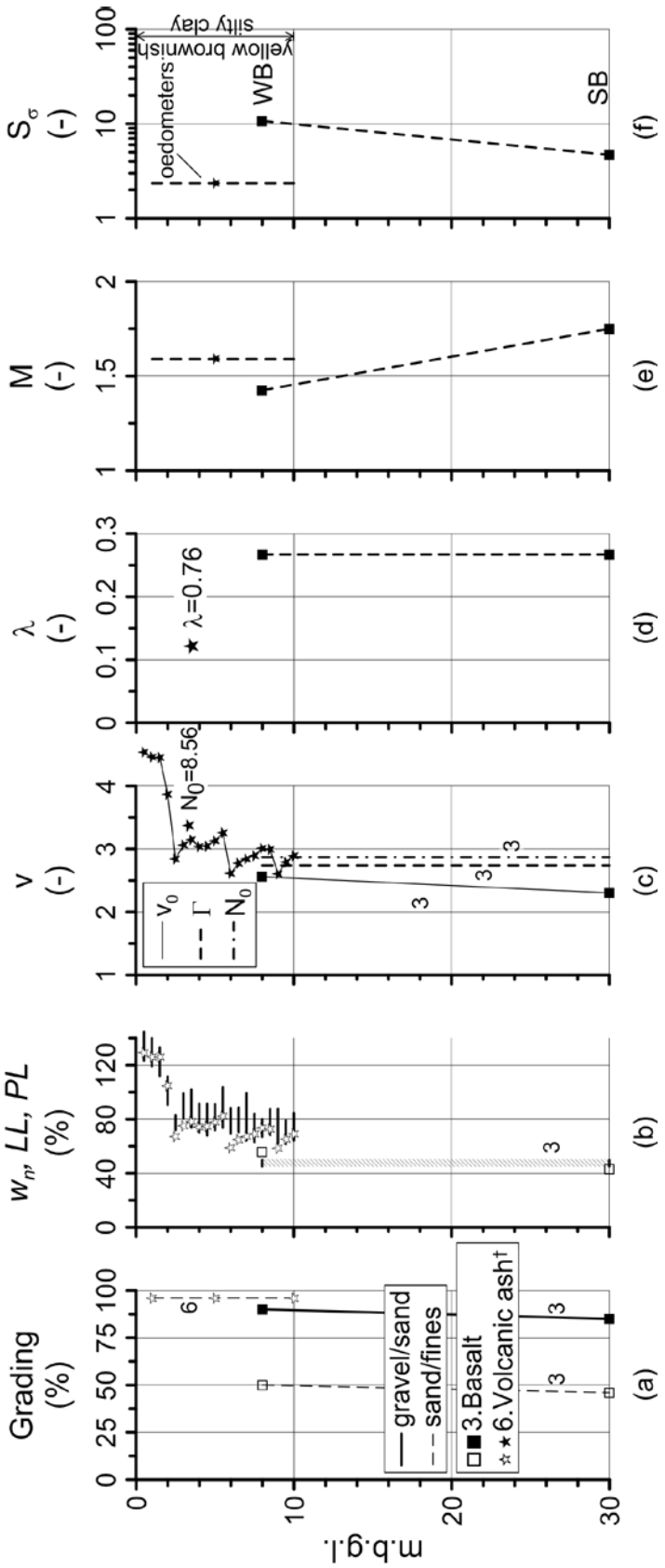

Figure 3: Comparison between the physical and mechanical characteristics of a basalt from Mauritius (3) and a volcanic ash residual soil from Java (6), Indonesia. †Data from Wesley (1973)

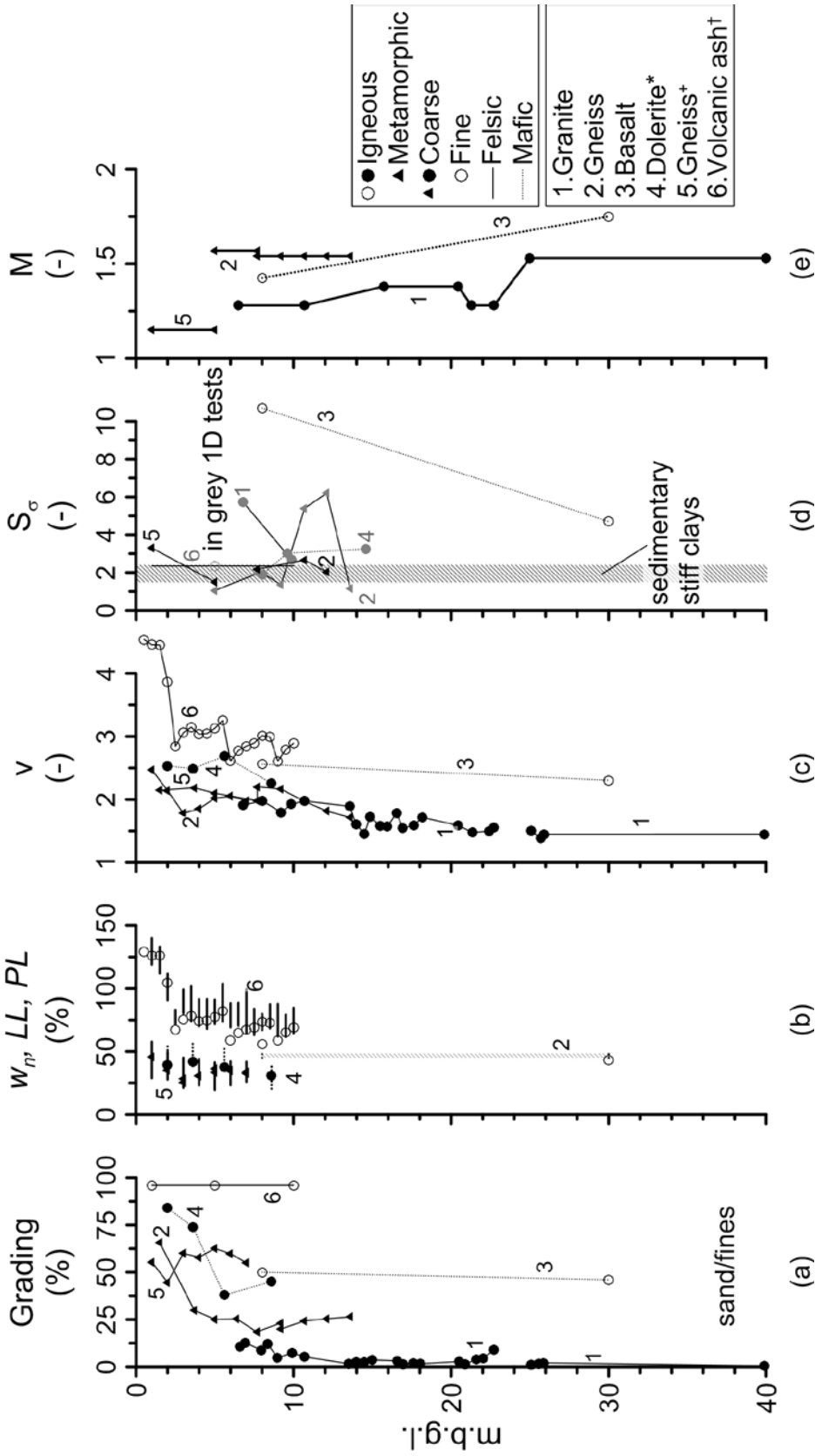

Figure 4: Comparison of physical and mechanical properties for a number of weathered geomaterials. 1.Granite, 2.Gneiss, 3.Basalt, 4.Dolerite (*data from Maccarini et al., 1989), 5.Gneiss (+data from Futai et al., 2004), 6. Volcanic ash residual soil (†data from Wesley, 1973)

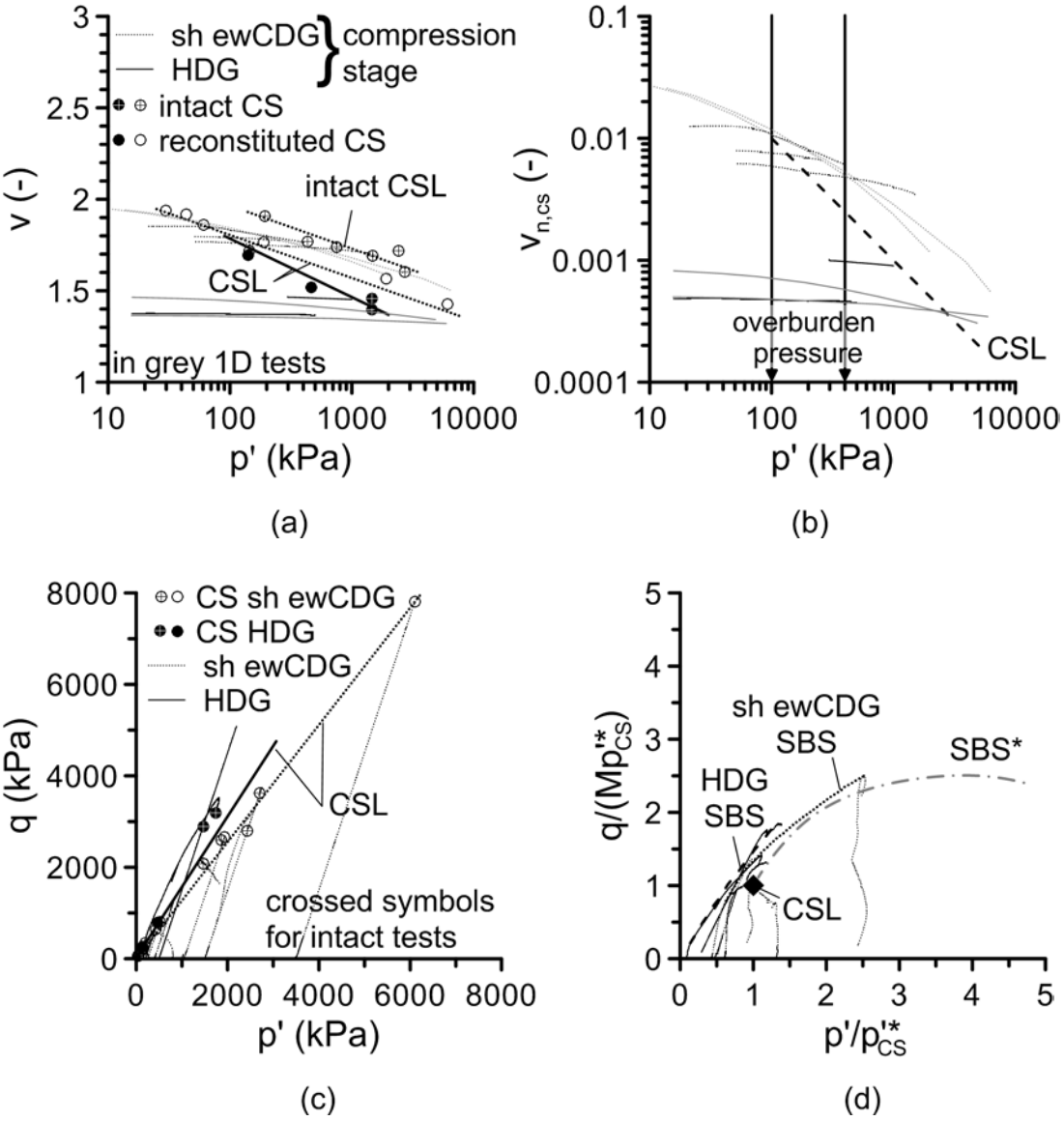

Figure 5: Granitic saprolite: (a) isotropic and 1D- compression tests on intact samples and CSLs, (b) normalised compression tests, (c) triaxial tests and CSLs and (d) SBSs (data as in Rocchi & Coop, 2015)

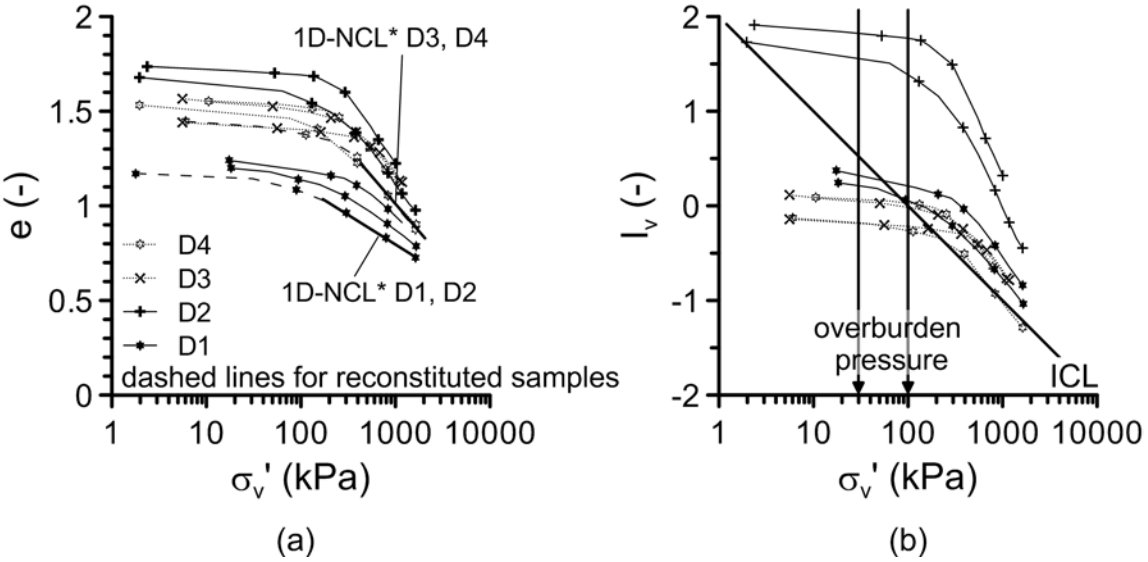

Figure 6: Doleritic saprolite: (a) 1D-compression tests on intact samples and 1D-NCL*s and (b) normalised compression tests (data from Maccarini et al., 1989)

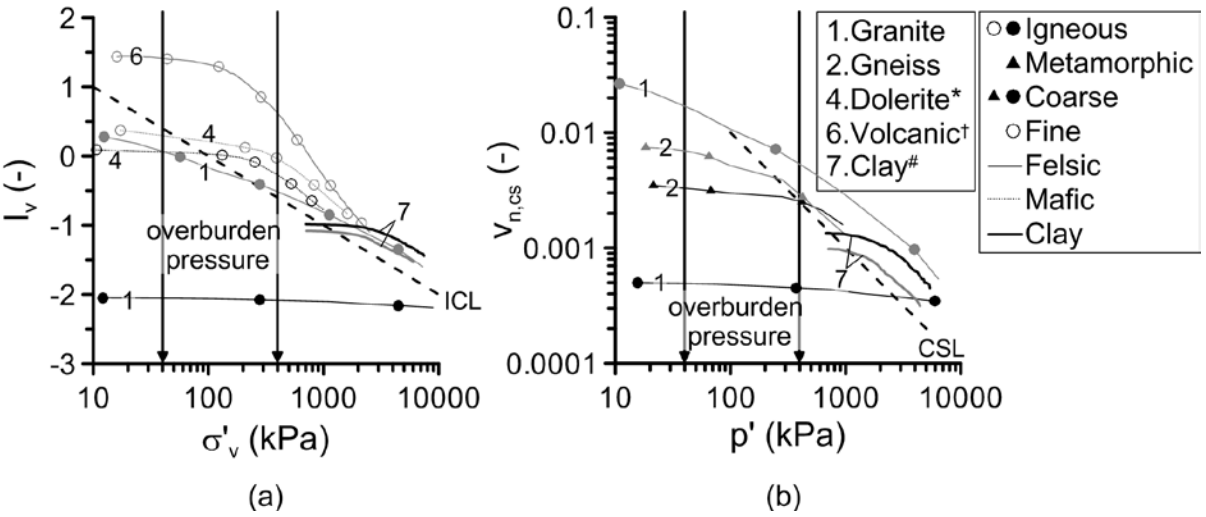

Figure 7: Comparison of the normalised one-dimensional compression tests for a number of weathered geomaterials. 1.Granite, 2.Gneiss, 4.Dolerite (data from Maccarini et al., 1989), 5.Gneiss ([+]data from Futai et al., 2004), 6.Volcanic ash residual soil ([†]data from Wesley, 1990) 7.Clay ([#]data from Cafaro & Cotecchia, 2001). (a) Void Index plane and (b) $v_{n,CS}$ plane.

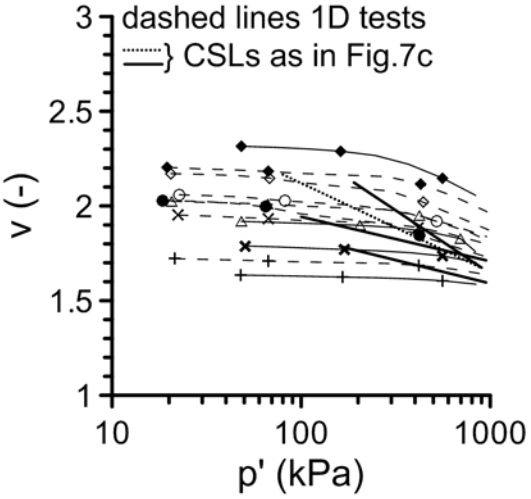
dashed lines 1D tests
} CSLs as in Fig.7c
v (-)
p' (kPa)

(a)

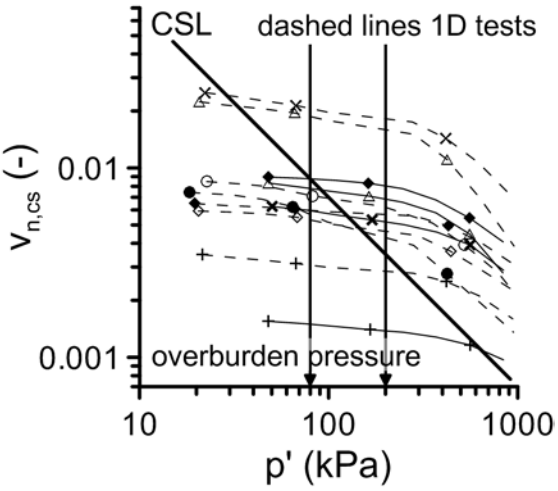
CSL
dashed lines 1D tests
$v_{n,cs}$ (-)
overburden pressure
p' (kPa)

(b)

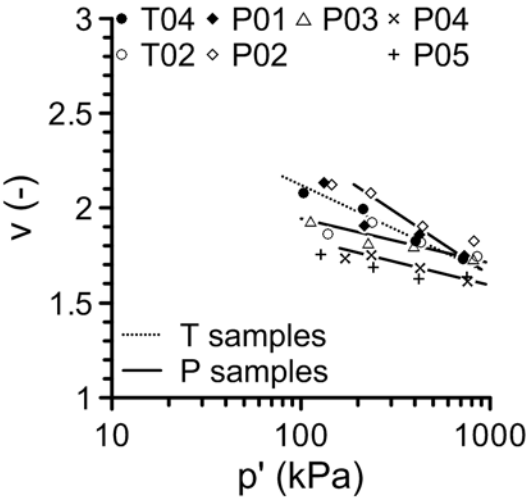
T04 P01 P03 P04
T02 P02 P05
T samples
P samples
v (-)
p' (kPa)

(c)

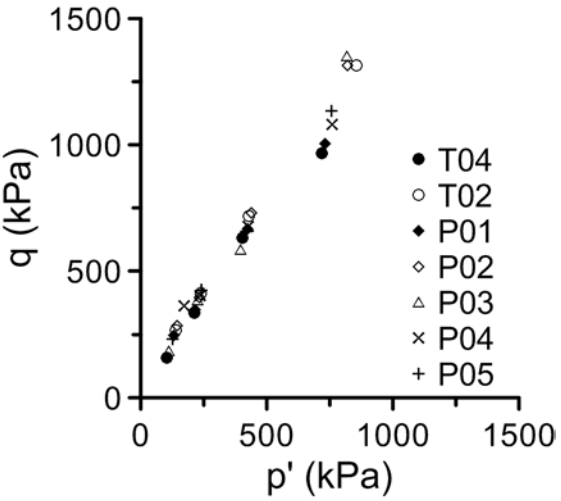
T04
T02
P01
P02
P03
P04
P05
q (kPa)
p' (kPa)

(d)

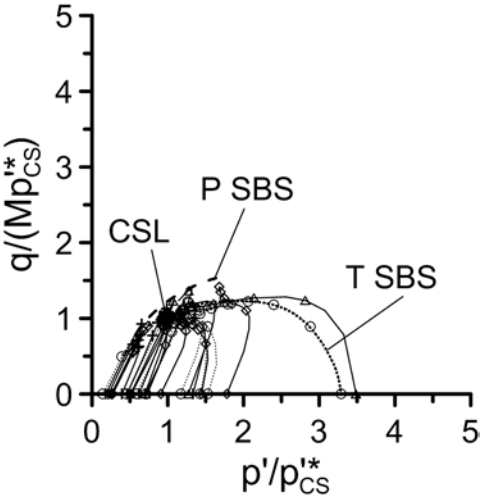
P SBS
CSL
T SBS
$q/(Mp'^*_{CS})$
p'/p'^*_{CS}

(e)

Figure 8: Gneissic saprolite: (a) critical states and CSLs (b) isotropic and 1D- compression tests, (c) critical states in a stress plane, (d) normalised isotropic and 1D- compression tests and (e) SBS (data from Maccarini, 1987)

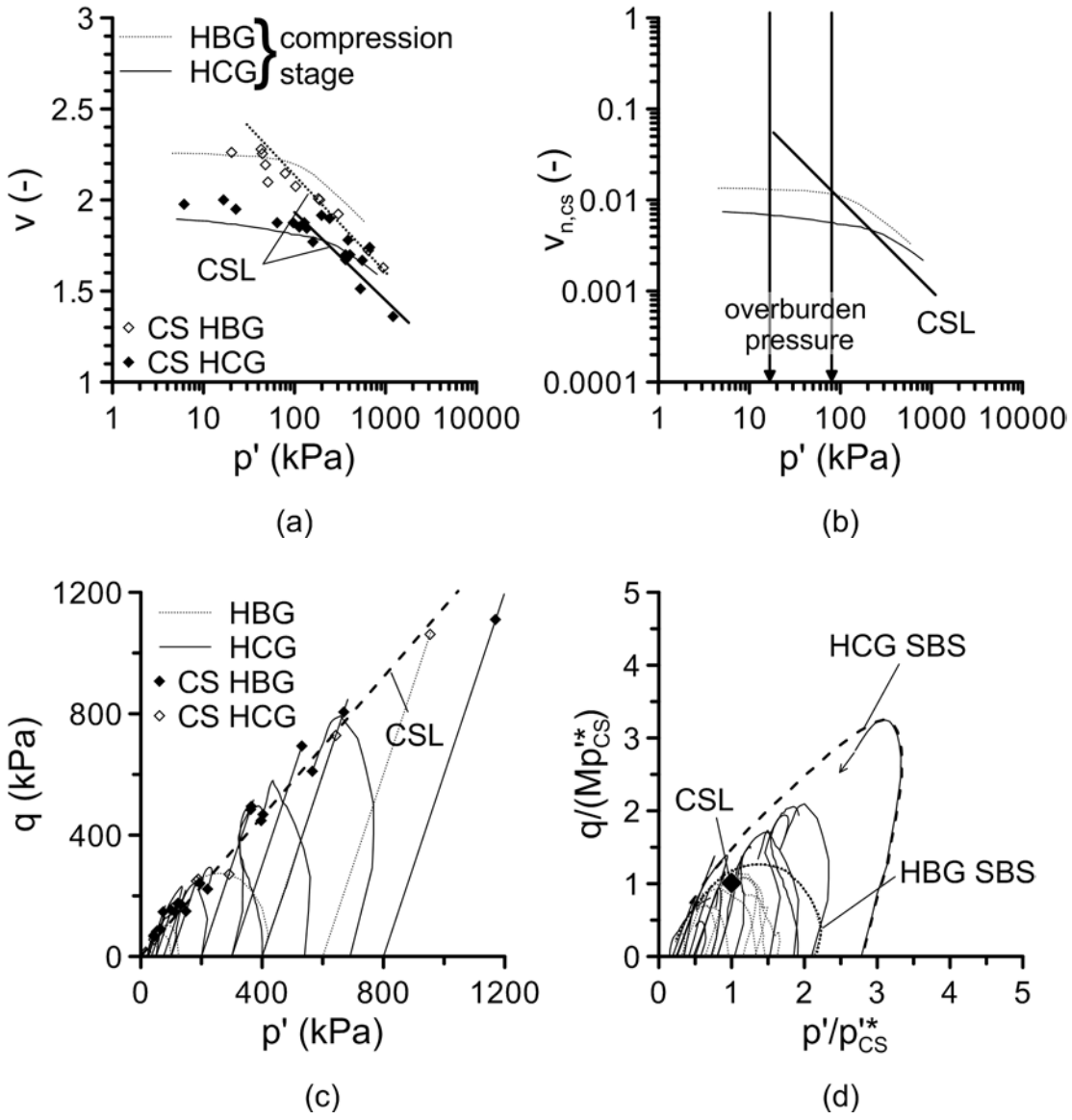

Figure 9: Gneissic saprolite: (a) isotropic compression tests on intact samples and CSLs, (b) normalised isotropic compression tests, (c) triaxial tests and CSLs and (d) SBSs (data from Futai et al., 2004)

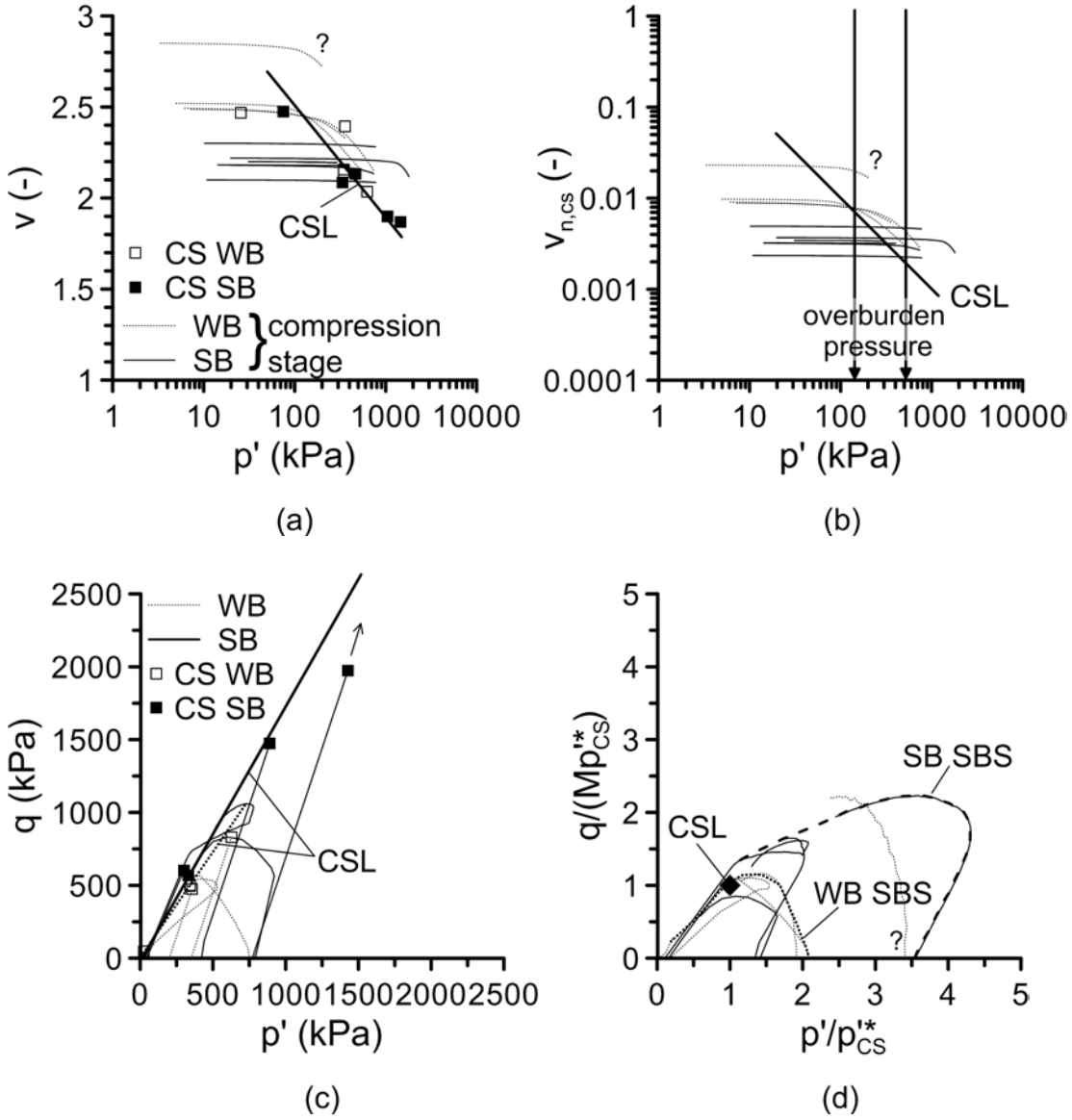

Figure 10: Basaltic saprolite: (a) isotropic compression tests on intact samples and CSLs, (b) normalised compression tests, (c) triaxial tests and CSLs and (d) SBSs (data from Maccarini, 1987)

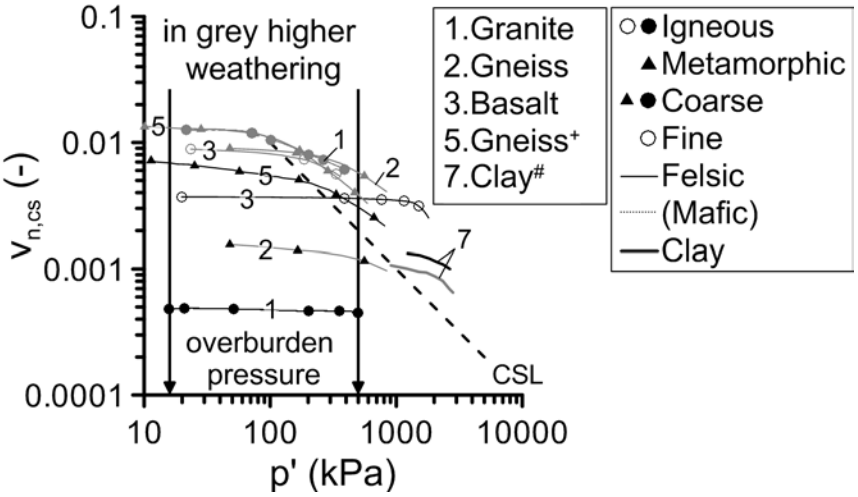

Figure 11: Comparison of the normalised isotropic compression tests for a number of weathered geomaterials. 1.Granite, 2.Gneiss, 3.Basalt, 5.Gneiss (+data from Futai et al., 2004), 7.Clay (#data from Cafaro & Cotecchia, 2001).

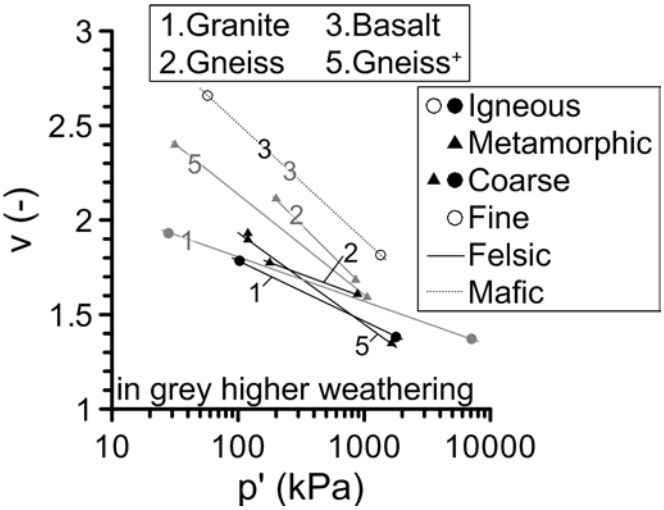

Figure 12: Comparison of the CSLs for a number of weathered geomaterials. 1.Granite, 2.Gneiss, 3.Basalt, 5.Gneiss (+data from Futai et al., 2004).

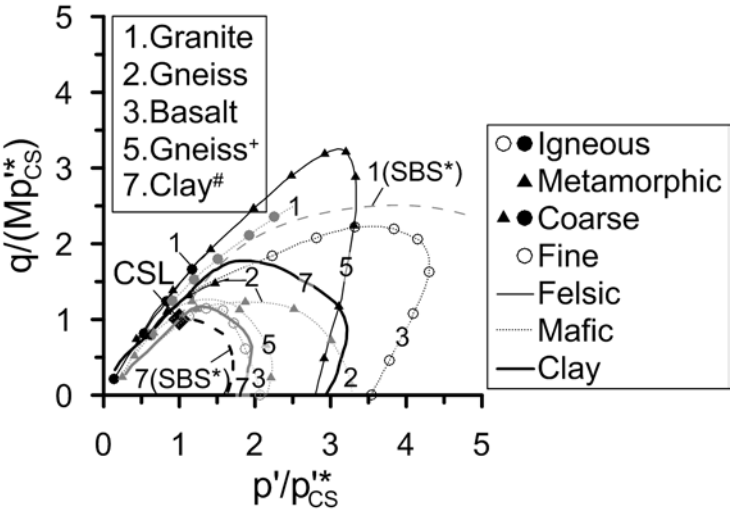

Figure 13: Comparison of the SBSs for a number of weathered geomaterials. 1.Granite, 2.Gneiss, 3.Basalt, 5.Gneiss ([+]data from Futai et al., 2004), 7.Clay ([#]data from Cafaro & Cotecchia, 2001).